

Contents lists available at ScienceDirect

Vision Research





Quantum Mechanics/Molecular mechanics calculations predict A1, not A2, is present in melanopsin (Opn4m) of red-eared slider turtles (*Trachemys scripta elegans*)

Michael S. O'Connor^{a,1}, Zoey T. Bragg^a, James R. Dearworth Jr.^b, Heidi P. Hendrickson^{a,*}

ARTICLE INFO

Keywords: Melanopsin (Opn4m) Red-eared slider turtles 11-cis-retinal (A1) 11-cis-dehydroretinal (A2) quantum mechanics/molecular mechanics (QM/MM) time-dependent density functional theory (TDDFT)

ABSTRACT

Melanopsin is a photopigment that plays a role in non-visual, light-driven, cellular processes such as modulation of circadian rhythms, retinal vascular development, and the pupillary light reflex (PLR). In this study, computational methods were used to understand which chromophore is harbored by melanopsin in red-eared slider turtles (Trachemys scripta elegans). In mammals, the vitamin A derivative 11-cis-retinal (A1) is the chromophore, which provides functionality for melanopsin. However, in red-eared slider turtles, a member of the reptilian class, the identity of the chromophore remains unclear. Red-eared slider turtles, similar to other freshwater vertebrates, possess visual pigments that harbor a different vitamin A derivative, 11-cis-3,4-didehydroretinal (A2), making their pigments more sensitive to red-light than blue-light, therefore, suggesting the chromophore to be the A2 derivative instead of the A1. To help resolve the chromophore identity, in this work, computational homology models of melanopsin in red-eared slider turtles were first constructed. Next, quantum mechanics/ molecular mechanics (QM/MM) calculations were carried out to compare how A1 and A2 derivatives bind to melanopsin. Time dependent density functional theory (TDDFT) calculations were then used to determine the excitation energy of the pigments. Lastly, calculated excitation energies were compared to experimental spectral sensitivity data from responses by the irises of red-eared sliders. Contrary to what was expected, our results suggest that melanopsin in red-eared slider turtles is more likely to harbor the A1 chromophore than the A2. Furthermore, a glutamine (Q62^{2.56}) and tyrosine (Y85^{3.28}) residue in the chromophore binding pocket are shown to play a role in the spectral tuning of the chromophore.

1. Introduction

Opsin photopigments are a special type of G-protein coupled receptor protein that convert light to a biochemical signal via a covalently-bound chromophore. Opsins are mostly present in the photoreceptor cells in the retina: cones (conopsins) for colored light and rods (rhodopsins) for brightness. Melanopsins (Opn4) are another branch of opsins (Provencio et al., 1998; Kumbalasiri et al., 2007) with close homology to cephalopod opsins (Provencio et al., 1998; Terakita et al., 2012). Like other opsins, melanopsin consists of seven transmembrane alpha helices (Provencio et al., 1998). Melanopsin in turtles, in particular, is predicted to possess a uniquely long cytoplasmic tail with the potential for many phosphorylation sites (Cheng et al., 2017).

In typical opsins, the binding pocket contains a vitamin A derivative in the 11-cis configuration that acts as a chromophore (Palczewski et al., 2000; Okada et al., 2004; Murakami & Kouyama, 2008; Park et al., 2013). Once the chromophore absorbs a photon, it isomerizes to the all-trans conformation (El-Tahawy et al., 2018; Gozem et al., 2012; Sekharan et al., 2012; Marín et al., 2019). This isomerization creates a conformational shift of the protein which initiates a signal transduction pathway that eventually sends a signal to the brain or muscle cells.

Since the discovery of melanopsin, two orthologs have been found for this protein, mammalian (Opn4m) and non-mammalian (Opn4x) (Bellingham et al., 2006; Peirson et al., 2009; Porter et al., 2012). They have evolved throughout fish, amphibians, reptiles, birds, and mammals. Non-mammalian vertebrates (birds, reptiles, amphibians, and fish)

^a Department of Chemistry, Lafayette College, Easton, PA 18042, United States

b Department of Biology, Lafayette College, Easton, PA 18042, United States

^{*} Corresponding author.

E-mail address: hendrihe@lafayette.edu (H.P. Hendrickson).

Present Address: Department of Chemistry, The University of Wisconsin, Madison, WI 53706, United States.

have been found to have both forms while mammals only have the mammalian form. These two forms have been found to have significant differences in amino acid sequence, suggesting that they may perform different functions (Bellingham et al., 2006).

Melanopsin is involved in certain non-image forming processes, such as circadian rhythms and iris constriction, and is found to be expressed in retinal ganglion cells of mammals (Hattar et al., 2002; Lucas et al., 2001). In addition, melanopsin has been found to be expressed in the retina and iris tissue (Provencio et al., 2000; Provencio et al., 1998; Xue et al., 2011). Originally, melanopsin was not thought to be involved in image forming but recent studies have shown otherwise (Sondereker et al., 2020). Its expression in retinal and nonretinal tissues is suggestive of a role in both visual and non-visual photoreception (Provencio et al., 1998). Melanopsin mRNA has been isolated from irises and retinas of red-eared slider turtles (Cheng et al., 2017; Dearworth et al., 2011), although further studies are required to determine the tissue locations of where protein expression actually occurs.

In addition to the uncertainty of where melanopsin is expressed, it is not known what chromophore is present in the different forms of melanopsins in turtles. This study aims to determine the retinal chromophore that is likely to bind to the mammalian melanopsin in freshwater red-eared slider turtles. Based on other vertebrates, the melanopsin binding pocket consists of a retinal chromophore bound to a lysine residue forming a protonated Schiff base (PSB) complex (Sekharan et al., 2012). In turtles, the chromophore could be one of two vitamin A derivatives: 11-cis-retinal (A1) or 11-cis-3,4-didehydroretinal (A2), structures shown in Fig. 1 (Liebman & Granda, 1971; Liebman, 1972).

The two potential chromophores are nearly identical in structure except that the A2 has an extra double bond in the β -ionone ring, which extends the π -conjugated chain. The additional double bond in the A2 chromophore allows the molecule to absorb lower energy photons than the A1 chromophore, thus red-shifting the absorption wavelength. Water is normally blue, but freshwater environments typically have brownish-red water due to the tannins from decaying leaves (Lee et al., 2003; Archetti et al., 2009). Since these tannins reflect red wavelengths, the water has a red tint compared to water without any tannins. Therefore, animals in this environment may be more likely to have A2 due to the environmental pressures, which require a molecule that can absorb reddish light. On the other hand, saltwater does not typically have these tannins and is more blue in color (Braun & Smirnov, 1993). As a result, animals in marine environments require a molecule that absorbs more blueish light and would be more likely to evolve proteins with A1. Salmon are a good example of the chromophore dependence on environmental pressure. Salmon have been found to contain both A1 and A2 in their rhodopsins. These organisms spend part of their life in freshwater and the other part in saltwater. When they are in freshwater their rhodopsins are found to contain A2 and when they are in saltwater their rhodopsins contain A1 (Enright et al., 2015). Freshwater turtles

Fig. 1. Structure of the (A) 11-cis-retinal (A1) and (B) 11-cis-dehydroretinal (A2) chromophores bound to a lysine residue via a protonated Schiff base linkage.

11-cis-dehydroretinal (A2)

have also been found to have A2 chromophores in their visual opsins, while marine turtle species have A1 in their visual opsins (Liebman & Granda, 1971; Liebman, 1972).

The hypothesis driving the work presented here was that, due to its freshwater environment, the melanopsin of red-eared slider turtles contains the A2 chromophore. Previous work suggested A2 is present in melanopsin of red-eared slider turtles based on a spectral sensitivity study (Sipe et al., 2011). However, more recent work suggests that A1 is present for melanopsin in the iris and A2 is present for melanopsin in the retina (Cheng et al., 2017). To resolve this issue, homology models of melanopsin for red-eared slider turtles containing each chromophore were constructed and investigated using quantum mechanics/molecular mechanics (QM/MM) calculations and time-dependent density functional theory (TDDFT). The calculated excitation energies were compared to experimental spectral sensitivity data from responses by the irises of red-eared slider turtles.

2. Methods

2.1. Homology model

The melanopsin homology model was generated using SWISS-MODEL, a homology modeling website and database (Guex et al., 2009; Benkert et al., 2011; Bertoni et al., 2017; Bienert et al., 2017; Waterhouse et al., 2018). An amino acid sequence is provided as input, and based on the sequence, a template crystal structure in the protein data bank (PDB) is identified. SWISS-MODEL uses BLAST to find sequences that are the most similar to the input sequence. BLAST is an algorithm that searches databases for protein or DNA sequence similarities. It uses an arbitrary position-specific score matrix in association with a substitution matrix for amino acids of similar chemical properties (Altschul et al., 1997). Once a sequence has been inputted, a list of templates is generated and ranked based on similarity to the input sequence. The partial amino acid sequence of the mammalian melanopsin, Opn4m, covering the transmembrane region of the protein (UniProt Accession Number: E7CL04, 334 amino acids) (Dearworth et al., 2011) for red-eared slider turtles was inputted into SWISS-MODEL and a list of templates was generated. From this list of templates the squid rhodopsin crystal structure (PDB ID: 2z73) was selected (Murakami & Kouyama, 2008). Since melanopsin shares a close homology with cephalopod opsins, the squid rhodopsin template was the best choice to create the melanopsin homology model (Provencio et al., 1998; Terakita et al., 2012).

The squid rhodopsin template covered from D3^{1.26} to P304^{8.59} and the other amino acids were excluded from the model, as shown in Fig. 2. The Ballesteros-Weinstein (BW) numbering is used to describe the amino acid numbers in both squid rhodopsin and red-eared slider turtle mammalian melanopsin sequences (Ballesteros & Weinstein, 1995). The homology model was then generated using template-based fragment assembly available in SWISS-MODEL, based on the sequence alignment between squid rhodopsin and the mammalian melanopsin for red-eared slider turtles. The Global Model Quality Estimate (GMQE) score is a value from 0 to 1 that indicates the quality of the target-template alignment and is based on how well the template covers the target sequence, with higher values indicating better quality. The GMQE for the mammalian melanopsin model for red-eared slider turtles was 0.73. The QMEAN Z-score is another quality estimate based on how many standard deviations the model quality is from the quality of experimentally determined structures in the Protein Data Bank. Models with QMEAN below -4.0 should be rejected. The QMEAN score for the mammalian melanopsin model for red-eared slider turtles was -3.55, which is low, but within the range of quality models. For comparison, jumping spider rhodopsin (Varma et al., 2019) was also tested as a template due to close homology with melanopsin, however the resulting homology model had a QMEAN score of -3.98 and was rejected in favor of the squid rhodopsin model.

Target 2z73.1.A	TVDVPDHAHYTIGTVILVVGITGTLGNFLVIYAFCRSRSLRTPANMFIINLAISDFLMSITQA-PIFFTTSLHKHWIFGKQVPDAVYYSLGIFIGICGIIGCGGNGIVIYLFTKTKSLQTPANMFIINLAFSDFTFSLVNGFPLMTISCFLKKWIFGF
Target 2z73.1.A	KGCELYAFCGALFGITSMITLMAIALDRYFVITRPLASIVVMSKKKALIILLGVWLYSLAWSLPPFFGWSAYVPEGLLTS AACKVYGFIGGIFGFMSIMTMAMISIDRYNVIGRPMAASKKMSHRRAFIMIIFVWLWSVLWAIGPIFGWGAYTLEGVLCN
Target 2z73.1.A	CSWDYVTFTPSVRAYTMLLFCFVFFIPLIAIIYSYVFIFKAIKNTNEAVQNIGSDANKVSQRQYQRMKN-EWKMAKIALI CSFDYISRDSTTRSNILCMFILGFFGPILIIFFCYFNIVMSVSNHEKEMAAMAKRLNAKELRKAQAGANAEMRLAKISIV
Target 2z73.1.A	VILLYVISWSPYSVVALVAFAGYSHLLTPFMNTVPAVIAKASAIHNPIIYAITHPKYRMAIAKYVPCLRPLLRVSRKDSK IVSQFLLSWSPYAVVALLAQFGPLEWVTPYAAQLPVMFAKASAIHNPMIYSVSHPKFREAISQTFP
Target	SCSRYLSTRRSTVTSH

Fig. 2. SWISS-MODEL alignments of squid rhodopsin crystal structure (PDB ID: 2z73) with the mammalian melanopsin for red-eared slider turtles. The sequence for red-eared slider turtles is a partial sequence covering the transmembrane region (UniProt Accession Number: E7CL04, 334 amino acids). The template covers from D3^{1,26} to P304^{8,59} with a 41.72% sequence identity and 42% sequence similarity.

The A1 structure was added to the models after the protein structure was constructed. The chromophore geometry was taken from the squid rhodopsin crystal structure (PDB ID: 2z73) and added to the homology models using PyMOL to align the homology model and the crystal structure ("The PyMOL Molecular Graphics System, Version 2.0," n.d.). In order to construct the model with A2, the A1 structure was modified by creating a new double bond in the β -ionone ring, as shown in Fig. 1. To create the new double bond, one hydrogen was removed from each of the carbons involved in the double bond (specific carbon numbers are provided in the Supporting Information (SI), Figure S1). Waters identified in the squid rhodopsin crystal structure (Murakami & Kouyama, 2008) were also added to the homology model and were included in the subsequent calculations. An ACE (acetyl) cap was added to the N-terminus and NME (methylamine group) cap was added to the C-terminus for each protein model produced. PropKa3 was used to predict the protonation states of titratable amino acids (Olsson et al., 2011; Søndergaard et al., 2011). For all amino acids, except the K278^{7.42} bound to A1, the predicted pKas were typical, and no change to their typical protonation states at pH 7.0 was made. For K278^{7.42}, the pKa was predicted to be 6.75, however it was kept protonated in the model. K278^{7.42} is the well-known protonated Schiff base (PSB) covalently bound to the A1 chromophore, which is known to be protonated in opsins (and deprotonated upon activation) (Longstaff et al., 1986). It is possible that the covalent bond to A1 and the initial orientation of the β-ionone ring, which is known to have a significant effect on the pKa of the PSB (Zhu et al., 2013), could have led to the low pKa predicted for $K278^{7.42}$.

2.2. Quantum Mechanics/Molecular mechanics level of theory

The absorption of light by the chromophore must be modeled using a quantum mechanics (QM) approach, but the protein molecule is too large to describe the entirely with QM. Thus, a combined QM/MM approach was carried out for the melanopsin models for red-eared slider turtles. A QM/MM calculation is a multilayered calculation consisting of a high and low layer. Each layer is a selection of atoms in the system. The high layer is calculated at a higher level of theory (the QM region) and the lower layer is calculated at a lower level of theory (MM). The QM/MM calculations were performed using the ONIOM (our Own N-layer Integrated molecular Orbital molecular Mechanics) method provided via the Gaussian 16 software (Dapprich et al., 1999; Vreven et al., 2003, 2006; Frisch et al., 2016). The ONIOM method approximates the energy of the entire system by calculating the energy of the low layer, the energy of the high layer, and then subtracting the low layer energy contribution from high layer atoms.

The entire protein was calculated at the low level of theory. The low

layer utilized the AMBER (Assisted Model Building with Energy Refinement) force field parameters (Weiner & Kollman, 1981; Maier et al., 2015). For the A1 chromophore attached to the lysine residue, previously published parameters from a computational study on bovine rhodopsin were utilized (Altun et al., 2008a). In order to form the additional double bond on the β -ionone ring in A2, a hydrogen atom was removed from each carbon involved in that double bond. To adapt the A1 parameters to A2, the partial charges of the hydrogens that were removed were added to the charges of the carbons they were removed from. Details on the force field parameters for the A1 and A2 chromophores are provided in the SI Tables S1 & S2.

The high layer (QM region) consists of the chromophore atoms, the protonated Schiff base (PSB), and the epsilon and delta carbon (CE and CD) atoms of the lysine along with their hydrogens (Altun et al., 2008a). The QM calculations of the high layer were carried out using Density Functional Theory (DFT) (Hohenberg & Kohn, 1964; Kohn & Sham, 1965) at the CAM-B3LYP/6–311 + G(2d,p) level (Clark et al., 1983; Krishnan et al., 1980; McLean & Chandler, 1980; Yanai et al., 2004). This level of theory, and in particular the range-separated hybrid functional CAM-B3LYP, was previously shown to predict chromophore excited state properties that were in good agreement with high-level calculations based on configuration interaction (CI) theory, such as CASSCF, CASPT2/CASSCF, CC2, SORCI and MRCISD (Rostov et al., 2010).

When the high layer is covalently bonded to the low layer, as is the case for the opsins in this work, a link atom is required in order to complete the valence of all the atoms in the high layer calculation. The link atom is parameterized to be connected to an sp^3 carbon, so choosing a C–C bond as the high/low layer partition is recommended (Dapprich et al., 1999; Vreven et al., 2003). Partitioning the layers and adding a link atom to the positively charged nitrogen would cause polarization issues. Thus, the high layer was chosen to extend two carbons past the PSB nitrogen. The link atom was a hydrogen atom replacing the CG atom bound to the CD atom of the LYS.

2.3. Quantum Mechanics/Molecular mechanics calculations

The initial structure of each protein system was first optimized using an MM calculation, where all the atoms were treated with classical force field parameters (molecular mechanically). Next the geometry was optimized (quantum mechanically) at the CAM-B3LYP/6-31G(2d) level (Hehre et al., 1972; Hariharan & Pople, 1973, 1974; Gordon, 1980; Francl et al., 1982; Binning Jr. & Curtiss, 1990; Blaudeau et al., 1997; Rassolov et al., 1998, 2001; Ditchfield et al., 2003), then at the CAM-B3LYP/6-311G(2d,p) level (McLean & Chandler, 1980; Krishnan et al., 1980), and finally at the CAM-B3LYP/6-311 + G(2d,p) level (Clark

et al., 1983). Each of the QM/MM optimization calculations were conducted using mechanical embedding, where only the sterics – not the electrostatics – of the low layer region affects the optimization of the high layer. There were no constraints on any of the atoms in the calculations.

Following the set of three QM/MM geometry optimizations, a time-dependent DFT (TDDFT) calculation (Runge & Gross, 1984; Bauernschmitt & Ahlrichs, 1996; Casida et al., 1998; Stratmann et al., 1998; Van Caillie & Amos, 1999, 2000; Furche & Ahlrichs, 2002; Scalmani et al., 2006) was performed at the CAM-B3LYP/6–311 + G(2d,p) level. Electronic embedding was used for the TDDFT calculation, where the partial charges of atoms in the low layer affect the QM calculation of the high layer. In TDDFT, the excitation energy of the molecule is determined by using perturbation theory to simulate the molecule absorbing a photon of light. The excitation data provided from a TDDFT calculation – excitation energies and oscillator strengths – can be used to generate absorption spectra. In order to approximate the extinction coefficient that would be observed experimentally, the individual excitation energies (i.e., the stick spectrum) are broadened using the Gaussian broadening function provided in Equation (1) (Creating UV/Visible Plots)

$$\varepsilon_{i}(\widetilde{\nu}) = \varepsilon_{imax}(\widetilde{\nu}) \exp \left[-\left(\frac{\widetilde{\nu} - \widetilde{\nu}_{i}}{\sigma}\right)^{2} \right] \\
= \frac{\sqrt{\pi} \bullet e^{2} \bullet N_{A}}{1000 \bullet \ln(10) \bullet c^{2} \bullet m_{e}} \frac{f_{i}}{\sigma} \exp \left[-\left(\frac{\widetilde{\nu} - \widetilde{\nu}_{i}}{\sigma}\right)^{2} \right] \tag{1}$$

The excitation energy in wavenumbers, $\tilde{\nu}$, is the average value in the Gaussian distribution function and the standard deviation, σ , describes the width of the distribution. The constants in Eqn. (1) are Avogadro's number, N_A , the charge and mass of an electron, e and m_e , and the speed of light, c. The $\tilde{\nu}_i$ term corresponds to the energy of each individual excitation, i. The f_i term corresponds to the oscillator strength of each excitation, which is related to the transition dipole moment and represents the probability for the transition to occur. The total absorption spectrum is the sum of the extinction coefficients for all n individual excitations, as shown in Equation (2).

$$\varepsilon(\widetilde{\nu}) = \sum_{i=1}^{n} \varepsilon_i(\widetilde{\nu}) \tag{2}$$

In this work, the first 10 excited states were calculated for each model and were converted to extinction coefficients based on Equation (1). The total spectrum was then calculated according to Equation (2). The default value of σ provided in GaussView is 0.40 eV (Dennington et al., 2016) and was used in benchmarking the absorption of A1 in squid rhodopsin. However, a value of 0.35 eV was used for red-eared slider melanopsin to best model the spectral sensitivity (Sipe et al., 2011) observed in experiment. The value of σ was determined by finding the σ value that produced an absorption spectrum with the lowest mean absolute error compared to the spectral sensitivity data, as shown in the SI Figure S4.

Calculated excitation energies for A1 in squid rhodopsin were compared to experimental absorption maxima for A1, both in the gas phase and in squid rhodopsin (Knudsen et al., 2018; Shichida et al., 1979). To carry out gas phase (*in vacuo*) TDDFT calculations of the chromophore, the QM region, including the link atom, was taken out of the protein environment after the set of three QM/MM optimizations were performed on the full system, and then the chromophore structure was optimized in the gas phase. To take into account the effect of the protein environment on the structure of the chromophore, gas phase optimizations were carried out in two ways: 1) the geometry of the chromophore was frozen and only the position of the link atom (replaced with a hydrogen) was optimized, and 2) the positions of all chromophore atoms (including the link atom hydrogen) were optimized. Details of the

chromophore structures taken out of the protein are provided in the SI Table S3. After the gas phase optimizations, TDDFT calculations were carried out at the CAM-B3LYP/6–311 + G(2d,p) level.

Calculations were carried out on the Lafayette College shared high-performance computing cluster and the Extreme Science and Engineering Discovery Environment (XSEDE) (Towns et al., 2014).

3. Results and discussion

3.1. Benchmarking level of theory using squid rhodopsin

Calculated excitation energies and oscillator strengths for the $S_0 \rightarrow S_1$ transition are provided in Table 1 for all A1 molecular systems considered (other information about the chromophore structures and excitations are provided in the SI Tables S4-S8). Calculated excitation energy of the A1 chromophore using the CAM-B3LYP/6-311 + G(2d,p) level of theory were in agreement with the calculated literature value of 2.53 eV, which was calculated using the same level of theory (Rostov et al., 2010). As shown in Table 1, considering additional carbon atoms in the QM model does not have a significant effect on the absorption spectrum.

When the A1 chromophore is in the opsin binding pocket, there is an expected blueshift in the absorption energy. In bovine rhodopsin, the blueshift was found to result from a nearby glutamate that stabilizes the PSB (Ferré & Olivucci, 2003). In the melanopsin models, the PSB is stabilized by nearby tyrosine and glutamine residues, which are expected to have a similar electrostatic effect on the PSB nitrogen (as described in Section 3.2 below). To verify that the MM parameters used to describe the chromophores reproduce this expected blueshift in the protein environment, the calculated excitation energies for the chromophore *in vacuo* were compared to the calculated excitation energies for the chromophore in the protein environment. As shown in Table 1, in Fig. 3, and SI Figures S2 & S3, the calculated results are consistent with the expected blueshift from gas phase to protein environment.

Fig. 3 also shows the overestimation of the calculated excitation energy compared to experiment. The overestimation is expected because although range-separated hybrid functionals like CAM-B3LYP provide a more accurate description of long-range excitations and correlate well with experimental values, they are known to slightly overestimate excitation energies (Jacquemin et al., 2014). As shown in Fig. 3A, the calculated absorption maximum for the A1 in the protein (blue) does not quantitatively agree with the corresponding experimentally observed absorption maximum (blue vertical line). In order to achieve quantitative agreement with experiment, the calculated excitation energies were shifted by -0.22 eV, which brings the calculated absorption maximum into alignment with the experimental value, as shown in Fig. 3B. The absorption spectrum of the retinal chromophore depends on the environment of the chromophore. In the case of squid rhodopsin, the overestimations of excitation energies are not consistent across chromophore environments. The calculated gas phase energies are more overestimated compared to experiment than the QM/MM (protein environment) energies, as evidenced in Fig. 3B, where the calculated and experimental maxima are aligned for the protein environment, but not for the gas phase environment. Since the calculations of melanopsin in this work are carried out in the protein environment (i.e., QM/MM calculations), it is most important that the calculated excitation energies agree well with the experimental value measured in the protein environment, thus the -0.22 eV shift was considered reasonable and was applied to calculations of melanopsin in this work.

3.2. Comparison between calculation and experiment for melanopsin of red-eared slider turtles

Previous work investigating the spectral sensitivity of the photointrinsic iris response in red-eared slider turtles examined the sensitivity of pupil constrictions to various wavelengths of light (Sipe et al., 2011). The data ranges from 410 to 640 nm. The relative sensitivity was

Table 1 Calculation summary for A1 in squid rhodopsin. Excitation energies (eV) and oscillator strengths corresponding to the $S_0 \rightarrow S_1$ transition are shown for different chromophore geometries in gas phase (*in vacuo*) and protein environments. Calculations were carried out at the CAM-B3LYP/6–311 + G(2d,p) level.

Chromophore Structure (shorthand)	Electronic Environment	Optimization Environment (Geometry)	Gas Phase Optimization constraint	Excitation Energy (eV)	Oscillator Strength
(sqrh-pPSB-2C)	Protein	Protein	None	2.76	1.27
(sqrh PSB)	Gas	Protein	Frozen geometry	2.47	1.02
(sqrh PSB-2C)	Gas	Protein	Frozen geometry	2.49	1.13
(PSB)	Gas	Gas	None	2.51	1.42
(PSB-2C)	Gas	Gas	None	2.53	1.51
(PSB-4C)	Gas	Gas	None	2.54	1.53

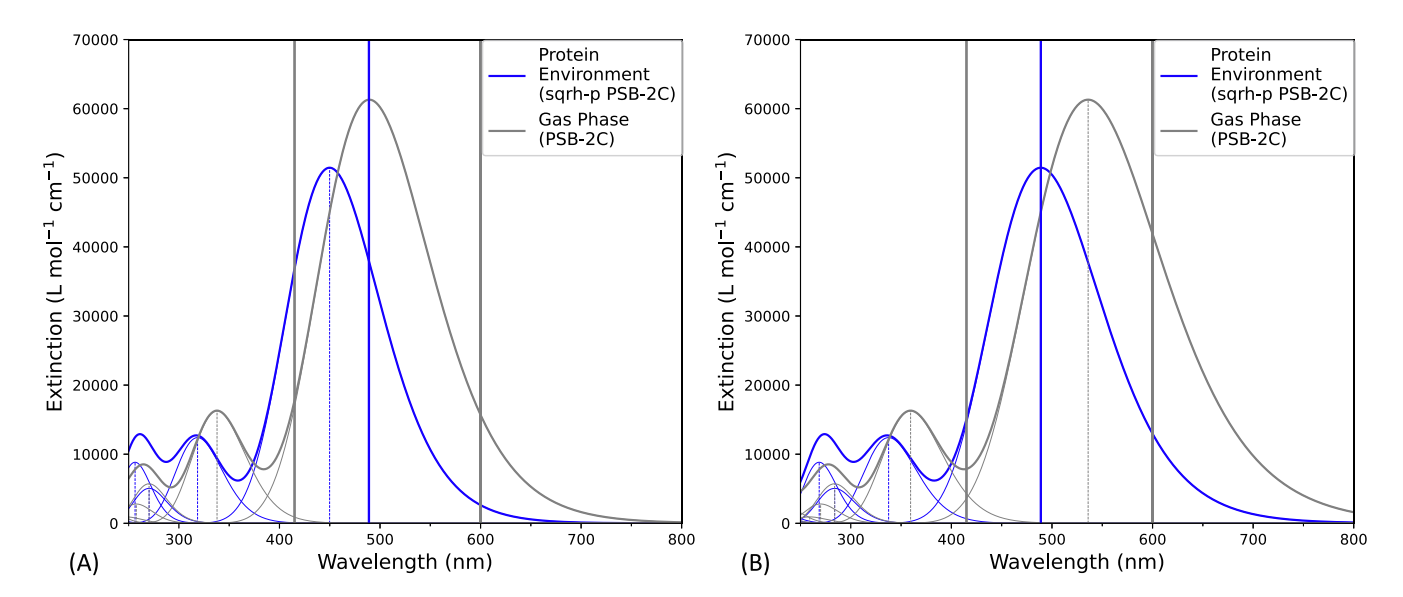


Fig. 3. Calculated absorption spectra for A1 gas phase (*in vacuo*, gray) and protein environment (QM/MM, blue). Shorthand from Table 1 is also included in parentheses for reference. Dotted vertical lines indicate the excitation wavelengths predicted by TDDFT. The solid vertical lines are experimental max values of 600 nm ($S_0 \rightarrow S_1$, gas phase), 415 nm ($S_0 \rightarrow S_2$, gas phase), and 489 nm ($S_0 \rightarrow S_1$, protein) (Knudsen et al., 2018; Shichida et al., 1979). (A) Calculated excitation energies. (B) Calculated excitation energies were shifted by -0.22 eV in order to align the absorption maxima for the calculated and experimental spectra in the protein environment.

determined by taking the log reciprocal of the threshold for photointrinsic iris response, in other words the amount of light that is required for the pupil to constrict. Since melanopsin was found to be the major driving force behind the pupil constriction (Dearworth et al., 2011; Sipe et al., 2011), measuring the pupil constriction at different wavelengths of light would be similar to measuring the absorption spectra of the melanopsin protein. The relative sensitivity was converted to a logarithmic scale and is plotted in Fig. 4 as black dots. Although the data point at 410 nm is thought to arise from cryptochrome (Sipe et al., 2011), it is shown here for completeness. While the 410 nm data point was considered in the present work, as described in the SI Figure S4, it does not affect the conclusions of this study.

The calculated extinction coefficient from the TDDFT calculations of the melanopsin models for red-eared slider turtles with A1 and A2 chromophores were converted to a logarithmic scale in order to compare to the experimental results and are plotted in Fig. 4. The calculated absorption maximum in Fig. 4 is shifted by -0.22 eV (based on the benchmarking with squid rhodopsin described above) and a broadening factor of 0.35 eV was applied to model the absorption line shape. The calculated absorption maxima are 477 nm and 504 nm for A1 and A2 models, respectively. (Raw, non-shifted calculated absorption data is provided in the SI Table S9.) These absorption maxima are in good agreement with the observed ranges of Opn4 absorption maxima measured for other species as well (Newman et al., 2003; Koyanagi et al., 2005; Qiu et al., 2005; Torii et al., 2007; Matsuyama et al., 2012; Sun et al., 2014; Tsukamoto et al., 2015). The calculated absorbance

spectrum for the A1 chromophore in melanopsin for red-eared slider turtles agrees better with the experimental photointrinsic iris response data than the spectrum for the A2 chromophore. The good agreement with experiment suggests that A1 is the chromophore present in the binding pocket of melanopsin in red-eared slider turtles, rather than A2.

To verify that minor differences in the value of the spectral shift do not impact the conclusions of this work, shifts in the range of 0.17 eV to 0.24 eV were also tested for melanopsin of red-eared slider turtles. Likewise, the broadening factor, i.e., standard deviation (σ), which is applied to model the line shape of the extinction coefficient, ϵ , can also affect how the calculated results compare to experiment, and broadening factors in the range of 0.25 eV to 0.45 eV were tested. Each shift and broadening factor were applied to calculate the extinction coefficient, which was then normalized by dividing by the maximum value of ϵ . The log of the normalized value was then compared to the experimental spectral sensitivity. For each calculated spectrum, the absolute value of the differences between each experimental data point and the calculated value were averaged to obtain the mean absolute error (MAE), which is plotted in Fig. 5.

The calculated spectrum with the smallest MAE agrees best with the experiment and indicates the shift and broadening factor that should be applied to model the experiment. As shown in Fig. 5, the optimum spectral shift is -0.23 eV with a broadening factor of 0.34 eV. In this work, a spectral shift of -0.22 eV with broadening factor of 0.35 eV, which also has a near-minimum MAE compared to experiment, was chosen so that the shift is in agreement with the benchmarking for squid

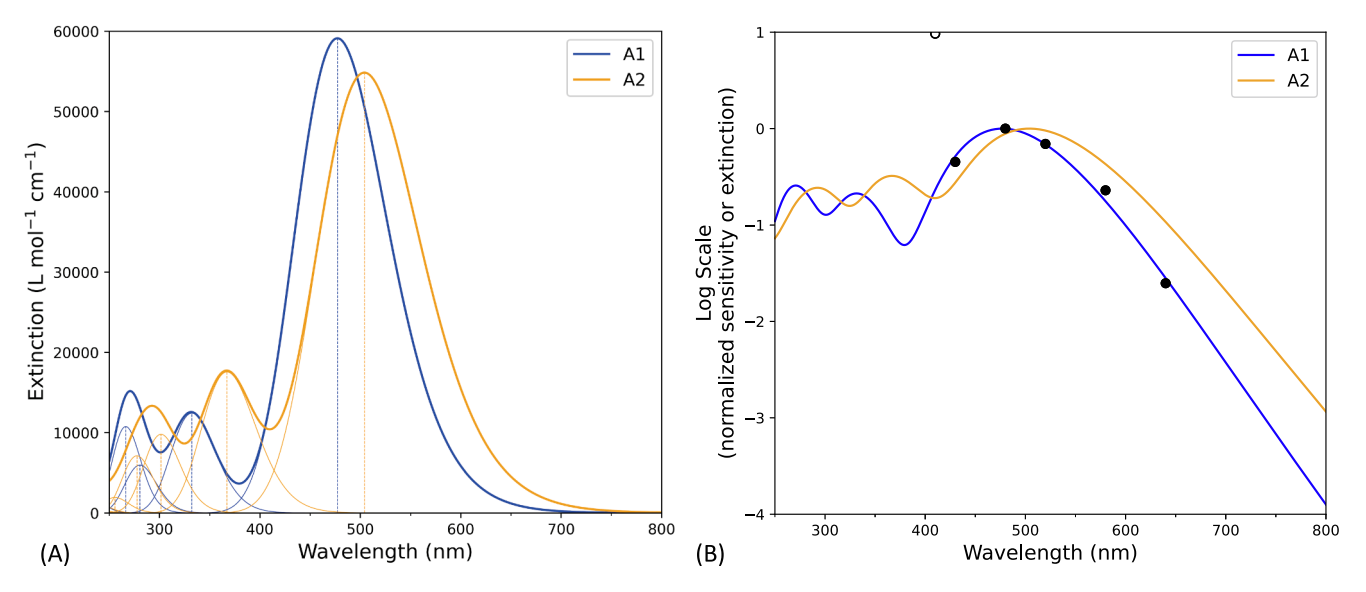


Fig. 4. (A) Calculated spectra of the mammalian melanopsin for red-eared slider turtles: A1 (blue) and A2 (orange) protein model. Calculated excitation energies are shown as dashed vertical lines that have been shifted by -0.22 eV. Artificial Gaussian broadening of 0.35 eV for each excitation is shown as thin solid lines. The overall spectrum for each model is shown as a thick solid line. (B) The calculated excitation energies were converted to a logarithmic scale to be directly compared to the experimental spectral sensitivity of melanopsin for red-eared slider turtles based on pupil constriction (black dots) (Sipe et al., 2011). The data point at 410 nm (black open circle) is expected to arise from cryptochrome, but is shown here for completeness (Sipe et al., 2011).

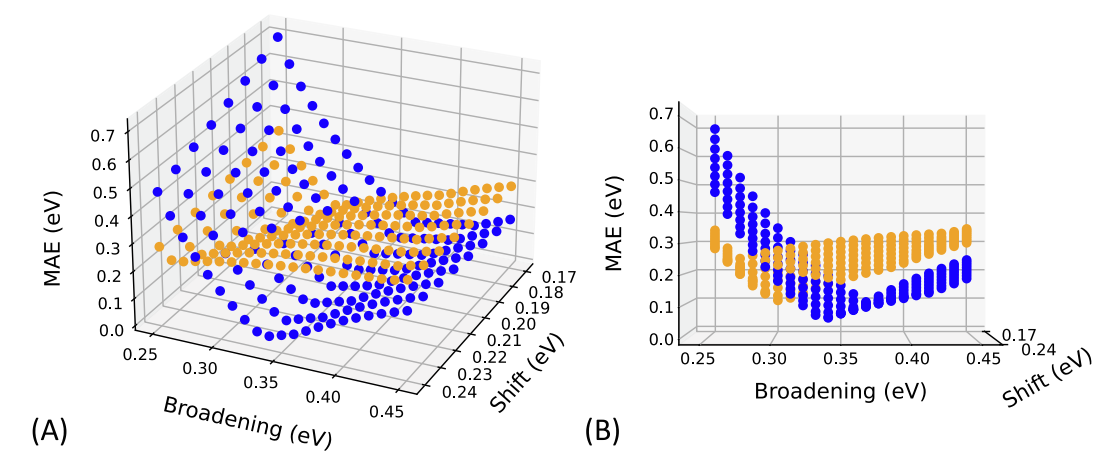


Fig. 5. Mean absolute error between the log of the calculated extinction coefficient and the experimental spectral sensitivity (Sipe et al., 2011) for a set of spectral shift and broadening factors applied to the calculated spectra for A1 (blue) and A2 (orange). (A) Angled view, (B) For clarity, a view straight down the spectral shift axis.

rhodopsin described in the previous section. However, we note that the conclusions of the study are the same for both of these parameter choices.

The differences between the A1 and A2 absorption spectra in melanopsin of red-eared slider turtles (Fig. 4) can be understood by examining the protein environment around the chromophore. The excitation energies for the $S_0 \rightarrow S_1$ transition for both chromophores in the protein environment and gas phase (*in vacuo*) are provided in Table 2, along with the differences between the A1 and A2 excitation energies (other excitations, oscillator strengths, natural transition orbitals, and structures are provided in SI Table S9-11). The excitation energy difference between A1 and A2 is smaller in the protein environment (-0.14 eV) than in the gas phase (-0.30 eV). As shown in Table 2, the protein environment blueshifts the absorption spectrum for the A2 chromophore more than for the A1 chromophore.

As discussed in the previous section, the excitation energy of the chromophore is expected to be blueshifted in the protein environment

Table 2Shifted excitation energies of A1 and A2 melanopsin models of red-eared slider turtles in the protein environment and gas phase, along with distance of surrounding residues to NZ of the PSB chromophore-LYS complex.

			A1	A2	Difference
Opn4m Residue	Oxygen Atom in Residue	Oxygen Partial Charge	Distance from NZ (Å)		
Q62 ^{2.56}	OE1	-0.6086	3.1	3.0	0.1
Y85 ^{3.28}	OH	-0.5579	3.3	3.2	0.1
E154 ^{ECL2}	OE2	-0.8188	3.7	3.8	-0.1
E154 ^{ECL2}	OE1	-0.8188	5.8	5.8	0.0
			Excitation Energy (eV)		
Protein Envir	Protein Environment				-0.14
Gas Phase En	2.32	2.02	-0.30		
Difference			0.28	0.44	0.16

compared to the gas phase (Ferré & Olivucci, 2003). While the

electrostatic interactions between the chromophore and the protein binding pocket involve many amino acid residues, in bovine rhodopsin the E113^{3.28} counterion residue is thought to have a significant contribution to the overall spectral shift (Fujimoto et al., 2007; Altun et al., 2008b; Fujimoto, 2021). In bovine rhodopsin, the electrostatic interaction between E113^{3.28} and the PSB^{7.42} shortens the hydrogen bond distance to the nitrogen, thus stabilizing the positive charge on the nitrogen, which contributes to a blueshift in the absorption spectrum (Ferré & Olivucci, 2003; Altun et al., 2008a, 2008b). In melanopsin of red-eared slider turtles, the calculated A1 and A2 structures show that a glutamine residue ($Q62^{2.56}$) is involved in the hydrogen bond network of the PSB^{7.42} nitrogen. The glutamine interacts with the PSB, and those electrostatic interactions may similarly stabilize the positive charge on the nitrogen and contribute to the observed blueshift in the chromophore absorption spectrum for the protein environment compared to the gas phase.

The distances between the Q62^{2.56} oxygen (OE1) and the PSB^{7.42} nitrogen (NZ) for melanopsin of red-eared slider turtles are recorded in Table 2 and are shown in Fig. 6. There is a smaller distance between the glutamine residue and the PSB for the A2 chromophore (3.0 Å) compared to A1 (3.1 Å), which provides evidence of a stronger interaction between the PSB and glutamine in the A2 structure. The stronger interaction could stabilize the positive charge on the PSB nitrogen, which may explain how the protein environment blueshifts the absorption spectrum for A2 more than for A1. Other nearby residues that could potentially have similar polarizing effects on the PSB include a tyrosine (Y85^{3.28}) and a glutamate (E154^{ECL2}), with distances also provided in Table 2. Y85^{3.28} is also closer to the PSB^{7.42} in A2 than in A1, indicating it would also stabilize the PSB in A2 more than in A1. On the other hand, E154^{ECL2} is actually farther away in the A2 structure than in A1, and would be expected to stabilize the PSB in A1 more than in A2.

As a result, we expect that $Q62^{2.56}$ and $Y85^{3.28}$ have a stronger combined effect on the PSB stabilization than E154^{ECL2}, and the stabilization results in a greater blueshift of the absorption spectrum for the A2 chromophore. Both $Q62^{2.56}$ and $Y85^{3.28}$ are neutral while E154^{ECL2} is anionic, but a simple point charge Coulomb analysis shows that it is indeed possible for the two neutral residues to have a stronger effect on the PSB than the anionic E154^{ECL2}, even though we do note the overall

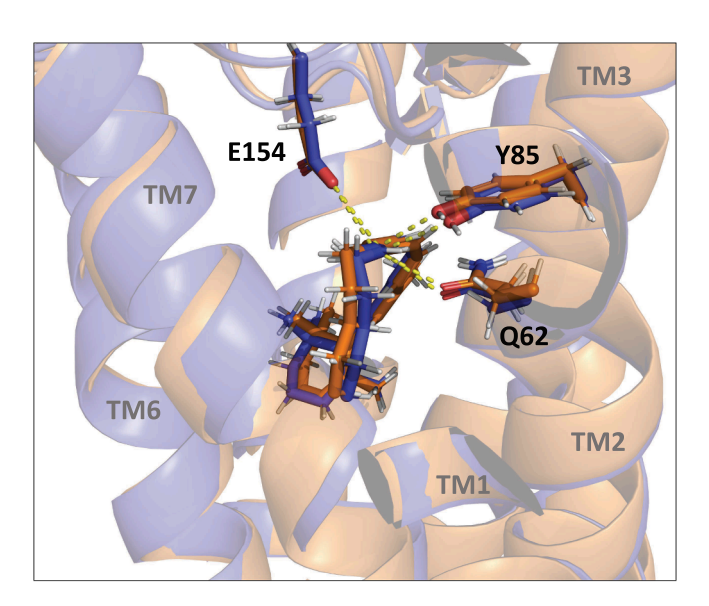


Fig. 6. Binding pocket of melanopsin model for red-eared slider turtles comparing structures with A1 (blue) and A2 (orange) chromophores. The labeled distances correspond to the distances between the $Q62^{2.56}$ OE1, Y85^{3.28} OH, and E154^{ECL2} OE2 atoms and the NZ atom of the PSB^{7.42} chromophore-LYS complex. Distances shown (yellow, dashed) are provided in Table 2.

electrostatic effect on the chromophore is due to the interaction of multiple amino acids (all atoms) surrounding the chromophore (Fujimoto et al., 2007; Fujimoto, 2021). In the simple analysis, the relative Coulomb potential at the PSB NZ nitrogen due to the oxygen atoms in Table 2 was determined by taking the sum of each oxygen partial charge divided by its distance from the NZ atom and then dividing the sum for $E154^{ECL2}$ by the sum for $Q62^{2.56}$ and $Y85^{3.28}$ combined. The negative potential due to $E154^{ECL2}$ is 99% and 95% that of $Q62^{2.56}$ and $Y85^{3.28}$ combined, for A1 and A2, respectively. Furthermore, in comparing the relative Coulomb potentials for A1 and A2, the potential from Q62^{2.56} and Y85^{3.28} combined is more negative for A2 than A1, and the potential from E154^{ECL2} is less negative for A2 than A1. Considering the magnitude of these relative increases and decreases in the negative potential from A1 and A2, the increase due to Q62^{2.56} and Y85^{3.28} is greater than the decrease due to E154^{ECL2}. This analysis indicates there is a smaller (less negative) potential present at the PSB nitrogen due to $E154^{ECL2}$ oxygen atoms than the $Q62^{2.56}$ and $Y85^{3.28}$ oxygen atoms. This simple analysis only points out the possible role of Q62^{2.56} and Y85^{3.28} in spectral tuning; it does not take into account the full electrostatic interaction due to binding site residues. Further investigations are currently underway in our lab to elucidate the relative importance of binding site residues on spectral tuning in melanopsin for red-eared slider turtles.

4. Conclusions

This work sought to determine whether the A1 or A2 chromophore is present in melanopsin of red-eared slider turtles using QM/MM and TDDFT calculations. It was hypothesized that the A2 chromophore would be present due to the freshwater environment of red-eared slider turtles and the presence of A2 in other freshwater turtle opsins. To test the hypothesis, a homology model of melanopsin for red-eared slider turtles was constructed based on the experimental structure of squid rhodopsin. The structure was optimized using the ONIOM QM/MM approach, and TDDFT calculations were carried out to determine the UV-Vis absorption energies of each chromophore. The calculated spectra were compared to experimental spectral sensitivity data based on the photointrinsic response of irises from red-eared slider turtles. The calculated absorption spectrum for A1 had a smaller mean absolute error compared to experimental values than for A2. Thus, the results of this study disagree with the initial hypothesis and indicate it is actually the A1 chromophore present in melanopsin of red-eared slider turtles.

The results of this study agree with the previous experimental observation of A1 in the iris (Cheng et al., 2017). However, other experimental results can also be explained by assuming A2 in the iris (Sipe et al., 2011). The calculations in the present study were carried out for Opn4m, but gene transcripts of both Opn4m and Opn4x have been found in the iris. Opn4x was not considered here because the full sequence of the transmembrane region of melanopsin in red-eared slider turtles is only available for Opn4m, not Opn4x. While Opn4m-with-A1 agrees well with the experimental spectral sensitivity for red-eared slider turtles, the calculations do not rule out the possibility that Opn4x-with-A2 could also agree well with experiment. We also acknowledge the comparison requires restraint since the pupil response curve from the photointrinsic iris response in red-eared turtles is a composite involving multiple photopigments not only including cryptochrome but also a combination of both Opn4x and Opn4m, each of which could even have different spectral properties (cf., in chicken (Torii et al., 2007)). Therefore, this study raises the question of how differences in Opn4x and Opn4m may affect which chromophore is present in the protein. This study also highlights the need to further test the general hypothesis that freshwater turtle melanopsin contains A2, while marine turtle melanopsin contains A1. Further investigation of differences between freshwater and marine turtle melanopsins, including both Opn4m and Opn4x, are the focus of ongoing investigations in our lab.

CRediT authorship contribution statement

Michael S. O'Connor: Conceptualization, Methodology, Investigation, Writing – original draft. Zoey T. Bragg: Validation, Investigation, Writing – original draft. James R. Dearworth Jr.: Conceptualization, Writing – review & editing. Heidi P. Hendrickson: Conceptualization, Methodology, Supervision, Project administration, Funding acquisition, Writing – review & editing.

Declaration of Competing Interest

The authors declare that they have no known competing financial interests or personal relationships that could have appeared to influence the work reported in this paper.

Data availability

Data will be made available on request.

Acknowledgements

Computational resources were provided in part by the MERCURY consortium (http://mercuryconsortium.org/) under NSF Grants CHE-1229354 and CHE-1662030. This work used the Extreme Science and Engineering Discovery Environment (XSEDE), which is supported by National Science Foundation grant number ACI-1548562. M.S.O. would like to acknowledge support from the Lafayette College Department of Biology Science Horizon Scholar Program and the Barry Goldwater Scholarship. M.S.O., Z.T.B. would like to acknowledge support from the Lafayette College EXCEL Scholars Program. M.S.O., Z.T.B., and H.P.H. thank Dr. Jason Simms and Peter Goode, Research Computing System Administrator, at Lafayette College for computational support.

References

- Altschul, S. F., Madden, T. L., Schäffer, A. A., Zhang, J., Zhang, Z., Miller, W., & Lipman, D. J. (1997). Gapped BLAST and PSI-BLAST: a new generation of protein database search programs. *Nucleic Acids Research*, 25, 3389–3402. https://doi.org/10.1093/nar/25.17.3389
- Altun, A., Yokoyama, S., & Morokuma, K. (2008a). Spectral Tuning in Visual Pigments: An ONIOM(QM:MM) Study on Bovine Rhodopsin and its Mutants. J. Phys. Chem. B, 112, 6814–6827. https://doi.org/10.1021/jp709730b
- Altun, A., Yokoyama, S., & Morokuma, K. (2008b). Mechanism of Spectral Tuning Going from Retinal in Vacuo to Bovine Rhodopsin and its Mutants: Multireference ab Initio Quantum Mechanics/Molecular Mechanics Studies. J. Phys. Chem. B, 112, 16883–16890. https://doi.org/10.1021/jp807172h
- Archetti, M., Döring, T. F., Hagen, S. B., Hughes, N. M., Leather, S. R., Lee, D. W., ... Thomas, H. (2009). Unravelling the evolution of autumn colours: An interdisciplinary approach. *Trends in Ecology & Evolution*, 24, 166–173. https://doi. org/10.1016/j.tree.2008.10.006
- Ballesteros, J. A., & Weinstein, H. (1995). Integrated methods for the construction of three-dimensional models and computational probing of structure-function relations in G protein-coupled receptors. In *Methods in Neurosciences* (pp. 366–428). Elsevier. https://doi.org/10.1016/S1043-9471(05)80049-7.
- Bauernschmitt, R., & Ahlrichs, R. (1996). Treatment of electronic excitations within the adiabatic approximation of time dependent density functional theory. *Chemical Physics Letters*, 256, 454–464. https://doi.org/10.1016/0009-2614(96)00440-X
- Bellingham, J., Chaurasia, S. S., Melyan, Z., Liu, C., Cameron, M. A., Tarttelin, E. E., ... Lucas, R. J. (2006). Evolution of Melanopsin Photoreceptors: Discovery and Characterization of a New Melanopsin in Nonmammalian Vertebrates. *PLoS Biol, 4*, e254.
- Benkert, P., Biasini, M., & Schwede, T. (2011). Toward the estimation of the absolute quality of individual protein structure models. *Bioinformatics*, 27, 343–350. https://doi.org/10.1093/bioinformatics/btq662
- Bertoni, M., Kiefer, F., Biasini, M., Bordoli, L., & Schwede, T. (2017). Modeling protein quaternary structure of homo- and hetero-oligomers beyond binary interactions by homology. Sci Rep, 7, 10480. https://doi.org/10.1038/s41598-017-09654-8
- Bienert, S., Waterhouse, A., de Beer, T. A. P., Tauriello, G., Studer, G., Bordoli, L., & Schwede, T. (2017). The SWISS-MODEL Repository—new features and functionality. Nucleic Acids Res, 45, D313–D319. https://doi.org/10.1093/nar/gkw1132
- Binning, R. C., Jr., & Curtiss, L. A. (1990). Compact contracted basis sets for third-row atoms: Ga–Kr. Journal of Computational Chemistry, 11, 1206–1216. https://doi.org/ 10.1002/jcc.540111013

- Blaudeau, J.-P., McGrath, M. P., Curtiss, L. A., & Radom, L. (1997). Extension of Gaussian-2 (G2) theory to molecules containing third-row atoms K and Ca. J. Chem. Phys., 107, 5016–5021. https://doi.org/10.1063/1.474865
- Braun, C. L., & Smirnov, S. N. (1993). Why is Water Blue? *Journal of Chemical Education*, 70, 612–614
- Casida, M. E., Jamorski, C., Casida, K. C., & Salahub, D. R. (1998). Molecular excitation energies to high-lying bound states from time-dependent density-functional response theory: Characterization and correction of the time-dependent local density approximation ionization threshold. *The Journal of Chemical Physics*, 108, 4439–4449. https://doi.org/10.1063/1.475855
- Creating UV/Visible Plots from the Results of Excited States Calculations | Gaussian.com [WWW Document], (2017). URL https://gaussian.com/uvvisplot/ (accessed 5 26 22)
- Cheng, S., Dearworth, J. R., Esckilsen, S. J., Kubera, C. L., Anderson, C. R., Goldberg, L. A., ... Ho, E. (2017). Melanopsin mRNA in the Iris of Red-Eared Slider Turtles (Trachemys scripta elegans). Journal of Herpetology, 51, 538–551. https://doi. org/10.1670/16-046
- Clark, T., Chandrasekhar, J., Spitznagel, G. W., & Schleyer, P. V. R. (1983). Efficient diffuse function-augmented basis sets for anion calculations. III. The 3–21+G basis set for first-row elements, Li–F. *Journal of Computational Chemistry*, 4, 294–301. https://doi.org/10.1002/jcc.540040303
- Dapprich, S., Komáromi, I., Byun, K. S., Morokuma, K., & Frisch, M. J. (1999). A new ONIOM implementation in Gaussian98. Part I. The calculation of energies, gradients, vibrational frequencies and electric field derivatives1Dedicated to Professor Keiji Morokuma in celebration of his 65th birthday.1. Journal of Molecular Structure: THEOCHEM, 461–462, 1–21. https://doi.org/10.1016/S0166-1280(98)00475-8
- Dearworth, J. R., Selvarajah, B. P., Kalman, R. A., Lanzone, A. J., Goch, A. M., Boyd, A. B., ... Cooper, L. J. (2011). A mammalian melanopsin in the retina of a fresh water turtle, the red-eared slider (Trachemys scripta elegans). *Vision Research*, *51*, 288–295. https://doi.org/10.1016/j.visres.2010.10.025
- Dennington, R., Keith, T. A., Millam, J. M. (2016). GaussView 6.0.16.
- Ditchfield, R., Hehre, W. J., & Pople, J. A. (2003). Self-Consistent Molecular-Orbital Methods. IX. An Extended Gaussian-Type Basis for Molecular-Orbital Studies of Organic Molecules. *The Journal of Chemical Physics*, 54, 724. https://doi.org/ 10.1063/1.1674902
- El-Tahawy, M. M. T., Nenov, A., Weingart, O., Olivucci, M., & Garavelli, M. (2018). Relationship between Excited State Lifetime and Isomerization Quantum Yield in Animal Rhodopsins: Beyond the One-Dimensional Landau-Zener Model. J. Phys. Chem. Lett., 9, 3315–3322. https://doi.org/10.1021/acs.jpclett.8b01062
- Enright, J. M., Toomey, M. B., Sato, S., Temple, S. E., Allen, J. R., Fujiwara, R., ... Corbo, J. C. (2015). Cyp27c1 Red-Shifts the Spectral Sensitivity of Photoreceptors by Converting Vitamin A1 into A2. Current Biology, 25, 3048–3057. https://doi.org/ 10.1016/j.cub.2015.10.018
- Ferré, N., & Olivucci, M. (2003). Probing the Rhodopsin Cavity with Reduced Retinal Models at the CASPT2//CASSCF/AMBER Level of Theory. J. Am. Chem. Soc., 125, 6868–6869. https://doi.org/10.1021/ja035087d
- Francl, M. M., Pietro, W. J., Hehre, W. J., Binkley, J. S., Gordon, M. S., DeFrees, D. J., & Pople, J. A. (1982). Self-consistent molecular orbital methods. XXIII. A polarization-type basis set for second-row elements. J. Chem. Phys., 77, 3654–3665. https://doi.org/10.1063/1.444267
- Frisch, M. J., Trucks, G. W., Schlegel, H. B., Scuseria, G. E., Robb, M. A., Cheeseman, J. R., ... Fox, D. J. (2016). Gaussian 16, Revision B.01.
- Fujimoto, K., Hayashi, S., Hasegawa, J., & Nakatsuji, H. (2007). Theoretical Studies on the Color-Tuning Mechanism in Retinal Proteins. J. Chem. Theory Comput., 3, 605–618. https://doi.org/10.1021/ct6002687
- Fujimoto, K. J. (2021). Electronic Couplings and Electrostatic Interactions Behind the Light Absorption of Retinal Proteins. Front. Mol. Biosci., 8, Article 752700. https://doi.org/10.3389/fmolb.2021.752700
- Furche, F., & Ahlrichs, R. (2002). Adiabatic time-dependent density functional methods for excited state properties. *The Journal of Chemical Physics*, 117, 7433–7447. https://doi.org/10.1063/1.1508368
- Gordon, M. S. (1980). The isomers of silacyclopropane. *Chemical Physics Letters*, 76, 163–168. https://doi.org/10.1016/0009-2614(80)80628-2
- Gozem, S., Schapiro, I., Ferre, N., & Olivucci, M. (2012). The Molecular Mechanism of Thermal Noise in Rod Photoreceptors. Science, 337, 1225–1228. https://doi.org/ 10.1126/science.1220461
- Guex, N., Peitsch, M. C., & Schwede, T. (2009). Automated comparative protein structure modeling with SWISS-MODEL and Swiss-PdbViewer: A historical perspective. *ELECTROPHORESIS*, 30, S162–S173. https://doi.org/10.1002/elps.200900140
- Hariharan, P. C., & Pople, J. A. (1974). Accuracy of AH n equilibrium geometries by single determinant molecular orbital theory. *Molecular Physics*, 27, 209–214. https://doi.org/10.1080/00268977400100171
- Hariharan, P. C., & Pople, J. A. (1973). The influence of polarization functions on molecular orbital hydrogenation energies. *Theoret. Chim. Acta*, 28, 213–222. https://doi.org/10.1007/BF00533485
- Hattar, S., Liao, H.-W., Takao, M., Berson, D. M., & Yau, K.-M. (2002). Melanopsincontaining retinal ganglion cells: Architecture, projections, and intrinsic photosensitivity. *Science*, 295, 1065–1070. https://doi.org/10.1126/ science 1069609
- Hehre, W. J., Ditchfield, R., & Pople, J. A. (1972). Self—Consistent Molecular Orbital Methods. XII. Further Extensions of Gaussian—Type Basis Sets for Use in Molecular Orbital Studies of Organic Molecules. J. Chem. Phys., 56, 2257–2261. https://doi. org/10.1063/1.1677577
- Hohenberg, P., & Kohn, W. (1964). Inhomogeneous Electron Gas. *Phys. Rev.*, *136*, B864–B871. https://doi.org/10.1103/PhysRev.136.B864

- Jacquemin, D., Moore, B., Planchat, A., Adamo, C., & Autschbach, J. (2014).
 Performance of an Optimally Tuned Range-Separated Hybrid Functional for 0–0
 Electronic Excitation Energies. J. Chem. Theory Comput., 10, 1677–1685. https://doi.org/10.1021/ct5000617
- Knudsen, J. L., Kluge, A., Bochenkova, A. V., Kiefer, H. V., & Andersen, L. H. (2018). The UV-visible action-absorption spectrum of all-trans and 11-cis protonated Schiff base retinal in the gas phase. Phys. Chem. Chem. Phys., 20, 7190–7194. https://doi.org/ 10.1039/C7CP07512.J
- Kohn, W., & Sham, L. J. (1965). Self-Consistent Equations Including Exchange and Correlation Effects. Phys. Rev., 140, A1133–A1138. https://doi.org/10.1103/ PhysRev.140.A1133
- Koyanagi, M., Kubokawa, K., Tsukamoto, H., Shichida, Y., & Terakita, A. (2005). Cephalochordate Melanopsin: Evolutionary Linkage between Invertebrate Visual Cells and Vertebrate Photosensitive Retinal Ganglion Cells. Current Biology, 15, 1065–1069. https://doi.org/10.1016/j.cub.2005.04.063
- Krishnan, R., Binkley, J. S., Seeger, R., & Pople, J. A. (1980). Self-consistent molecular orbital methods. XX. A basis set for correlated wave functions. *The Journal of Chemical Physics*, 72, 650–654. https://doi.org/10.1063/1.438955
- Kumbalasiri, T., Rollag, M. D., Isoldi, M. C., Castrucci, A. M. de L., & Provencio, I. (2007). Melanopsin Triggers the Release of Internal Calcium Stores in Response to Light†: Photochemistry and Photobiology, 2007, 83. Photochemistry and Photobiology, 83, 273–280. https://doi.org/10.1562/2006-07-11-RA-964
- Lee, D. W., O'Keefe, J., Holbrook, N. M., & Feild, T. S. (2003). Pigment dynamics and autumn leaf senescence in a New England deciduous forest, eastern USA: Autumn leaf pigments. Ecological Research, 18, 677–694. https://doi.org/10.1111/j.1440-1703.2003.00588.x
- Liebman, P. A. (1972). Microspectrophotometry of photoreceptors. Handbook of Sensory Physiology., 481–528.
- Liebman, P. A., & Granda, A. M. (1971). Microspectrophotometric measurements of visual pigments in two species of turtle, Psuedemys scripta and Chleonia mydas. Vision Research, 11, 105–114.
- Longstaff, C., Calhoon, R. D., & Rando, R. R. (1986). Deprotonation of the Schiff base of rhodopsin is obligate in the activation of the G protein. *Proc. Natl. Acad. Sci. U.S.A.*, 83, 4209–4213. https://doi.org/10.1073/pnas.83.12.4209
- Lucas, R. J., Douglas, R. H., & Foster, R. G. (2001). Characterization of an ocular photopigment capable of driving pupillary constriction in mice. *Nat Neurosci*, 4, 621–626. https://doi.org/10.1038/88443
- Maier, J. A., Martinez, C., Kasavajhala, K., Wickstrom, L., Hauser, K. E., & Simmerling, C. (2015). ff14SB: Improving the Accuracy of Protein Side Chain and Backbone Parameters from ff99SB. J. Chem. Theory Comput., 11, 3696–3713. https://doi.org/10.1021/acs.ictc.5b00255
- Marín, M. del C., De Vico, L., Dong, S. S., Gagliardi, L., Truhlar, D. G., & Olivucci, M. (2019). Assessment of MC-PDFT excitation energies for a set of QM/MM models of rhodopsins. *Journal of Chemical Theory and Computation*, 15, 1915–1923. https://doi.org/10.1021/acs.ictc.8b01069
- Matsuyama, T., Yamashita, T., Imamoto, Y., & Shichida, Y. (2012). Photochemical Properties of Mammalian Melanopsin. *Biochemistry*, 51, 5454–5462. https://doi.org/ 10.1021/bi3004999
- McLean, A. D., & Chandler, G. S. (1980). Contracted Gaussian basis sets for molecular calculations. I. Second row atoms, Z=11-18. J. Chem. Phys., 72, 5639-5648. https://doi.org/10.1063/1.438980
- Murakami, M., & Kouyama, T. (2008). Crystal structure of squid rhodopsin. *Nature*, 453, 363–367. https://doi.org/10.1038/nature06925
- Newman, L. A., Walker, M. T., Brown, R. L., Cronin, T. W., & Robinson, P. R. (2003). Melanopsin Forms a Functional Short-Wavelength Photopigment. *Biochemistry*, 42, 12734–12738. https://doi.org/10.1021/bi035418z
- Okada, T., Sugihara, M., Bondar, A.-N., Elstner, M., Entel, P., & Buss, V. (2004). The Retinal Conformation and its Environment in Rhodopsin in Light of a New 2.2Å Crystal Structure. *Journal of Molecular Biology*, 342, 571–583. https://doi.org/ 10.1016/j.imb.2004.07.044
- Olsson, M. H. M., Søndergaard, C. R., Rostkowski, M., & Jensen, J. H. (2011). PROPKA3: Consistent Treatment of Internal and Surface Residues in Empirical p K a Predictions. J. Chem. Theory Comput., 7, 525–537. https://doi.org/10.1021/ct100578z
- Palczewski, K., Kumasaka, T., Hori, T., Behnke, C. A., Motoshima, H., Fox, B. A., ... Miyano, M. (2000). Crystal Structure of Rhodopsin. A G Protein-Coupled Receptor. Science, 289, 739–745. https://doi.org/10.1126/science.289.5480.739
- Park, J. H., Morizumi, T., Li, Y., Hong, J. E., Pai, E. F., Hofmann, K. P., ... Ernst, O. P. (2013). Opsin, a Structural Model for Olfactory Receptors? *Angew. Chem. Int. Ed.*, 52, 11021–11024. https://doi.org/10.1002/anie.201302374
- Peirson, S. N., Halford, S., & Foster, R. G. (2009). The evolution of irradiance detection: Melanopsin and the non-visual opsins. *Phil. Trans. R. Soc. B*, 364, 2849–2865. https://doi.org/10.1098/rstb.2009.0050
- Porter, M. L., Blasic, J. R., Bok, M. J., Cameron, E. G., Pringle, T., Cronin, T. W., & Robinson, P. R. (2012). Shedding new light on opsin evolution. *Proc. R. Soc. B*, 279, 3–14. https://doi.org/10.1098/rspb.2011.1819
- Provencio, I., Jiang, G., De Grip, W. J., Hayes, W. P., & Rollag, M. D. (1998). Melanopsin: An opsin in melanophores, brain, and eye. *Proceedings of the National Academy of Sciences*, 95, 340–345. https://doi.org/10.1073/pnas.95.1.340
- Provencio, I., Rodriguez, I. R., Jiang, G., Hayes, W. P., Moreira, E. F., & Rollag, M. D. (2000). A Novel Human Opsin in the Inner Retina. J. Neurosci., 20, 600–605. https://doi.org/10.1523/JNEUROSCI.20-02-00600.2000
- Qiu, X., Kumbalasiri, T., Carlson, S. M., Wong, K. Y., Krishna, V., Provencio, I., & Berson, D. M. (2005). Induction of photosensitivity by heterologous expression of melanopsin. *Nature*, 433, 745–749. https://doi.org/10.1038/nature03345

- Rassolov, V. A., Pople, J. A., Ratner, M. A., & Windus, T. L. (1998). 6–31G* basis set for atoms K through Zn. J. Chem. Phys., 109, 1223–1229. https://doi.org/10.1063/ 1.476673
- Rassolov, V. A., Ratner, M. A., Pople, J. A., Redfern, P. C., & Curtiss, L. A. (2001). 6–31G* basis set for third-row atoms. *Journal of Computational Chemistry*, 22, 976–984. https://doi.org/10.1002/jcc.1058
- Rostov, I. V., Amos, R. D., Kobayashi, R., Scalmani, G., & Frisch, M. J. (2010). Studies of the Ground and Excited-State Surfaces of the Retinal Chromophore using CAM-B3LYP. J. Phys. Chem. B, 114, 5547–5555. https://doi.org/10.1021/jp911329g
- Runge, E., & Gross, E. K. U. (1984). Density-Functional Theory for Time-Dependent Systems. Phys. Rev. Lett., 52, 997–1000. https://doi.org/10.1103/ Dhys. Descript 52.000.
- Scalmani, G., Frisch, M. J., Mennucci, B., Tomasi, J., Cammi, R., & Barone, V. (2006). Geometries and properties of excited states in the gas phase and in solution: Theory and application of a time-dependent density functional theory polarizable continuum model. *The Journal of Chemical Physics*, 124, Article 094107. https://doi.org/10.1063/1.2173258
- Sekharan, S., Wei, J. N., & Batista, V. S. (2012). The Active Site of Melanopsin: The Biological Clock Photoreceptor. J. Am. Chem. Soc., 134, 19536–19539. https://doi. org/10.1021/ia308763b
- Shichida, Y., Tokunaga, F., & Yoshizawa, T. (1979). SQUID HYPSORHODOPSIN. Photochem Photobiol, 29, 343–351. https://doi.org/10.1111/j.1751-1097.1979. tb07057.x
- Sipe, G. O., Dearworth, J. R., Selvarajah, B. P., Blaum, J. F., Littlefield, T. E., Fink, D. A., ... McDougal, D. H. (2011). Spectral sensitivity of the photointrinsic iris in the redeared slider turtle (Trachemys scripta elegans). Vision Research, 51, 120–130. https://doi.org/10.1016/j.visres.2010.10.012
- Sondereker, K. B., Stabio, M. E., & Renna, J. M. (2020). Crosstalk: The diversity of melanopsin ganglion cell types has begun to challenge the canonical divide between image-forming and non-image-forming vision. *J Comp Neurol*, 528, 2044–2067. https://doi.org/10.1002/cne.24873
- Søndergaard, C. R., Olsson, M. H. M., Rostkowski, M., & Jensen, J. H. (2011). Improved Treatment of Ligands and Coupling Effects in Empirical Calculation and Rationalization of p K a Values. J. Chem. Theory Comput., 7, 2284–2295. https://doi. org/10.1021/ct200133y
- Stratmann, R. E., Scuseria, G. E., & Frisch, M. J. (1998). An efficient implementation of time-dependent density-functional theory for the calculation of excitation energies of large molecules. *The Journal of Chemical Physics*, 109, 8218–8224. https://doi.org/ 10.1063/1.477483
- Sun, L., Kawano-Yamashita, E., Nagata, T., Tsukamoto, H., Furutani, Y., Koyanagi, M., & Terakita, A. (2014). Distribution of Mammalian-Like Melanopsin in Cyclostome Retinas Exhibiting a Different Extent of Visual Functions. *PLoS ONE*, 9, e108209.
- Terakita, A., Kawano-Yamashita, E., Koyanagi, M., 2012. Evolution and diversity of opsins. WIREs Membr Transp Signal 1, 104–111.
- The PyMOL Molecular Graphics System, Version 2.0, Schrödinger, LLC.
- Torii, M., Kojima, D., Okano, T., Nakamura, A., Terakita, A., Shichida, Y., ... Fukada, Y. (2007). Two isoforms of chicken melanopsins show blue light sensitivity. FEBS Letters, 581, 5327–5331. https://doi.org/10.1016/j.febslet.2007.10.019
- Towns, J., Cockerill, T., Dahan, M., Foster, I., Gaither, K., Grimshaw, A., ... Wilkins-Diehr, N. (2014). XSEDE: Accelerating Scientific Discovery. *Comput. Sci. Eng.*, 16, 62–74. https://doi.org/10.1109/MCSE.2014.80
- Tsukamoto, H., Kubo, Y., Farrens, D. L., Koyanagi, M., Terakita, A., & Furutani, Y. (2015). Retinal Attachment Instability Is Diversified among Mammalian Melanopsins. *Journal of Biological Chemistry*, 290, 27176–27187. https://doi.org/10.1074/jbc.M115.666305
- Van Caillie, C., & Amos, R. D. (2000). Geometric derivatives of density functional theory excitation energies using gradient-corrected functionals. *Chemical Physics Letters*, 317, 159–164. https://doi.org/10.1016/S0009-2614(99)01346-9
- Van Caillie, C., & Amos, R. D. (1999). Geometric derivatives of excitation energies using SCF and DFT. Chemical Physics Letters, 308, 249–255. https://doi.org/10.1016/ S0009-2614(99)00646-6
- Varma, N., Mutt, E., Mühle, J., Panneels, V., Terakita, A., Deupi, X., ... Lesca, E. (2019). Crystal structure of jumping spider rhodopsin-1 as a light sensitive GPCR. Proc. Natl. Acad. Sci. U.S.A., 116, 14547–14556. https://doi.org/10.1073/pnas.1902192116
- Vreven, T., Byun, K. S., Komáromi, I., Dapprich, S., Montgomery, J. A., Morokuma, K., & Frisch, M. J. (2006). Combining Quantum Mechanics Methods with Molecular Mechanics Methods in ONIOM. J. Chem. Theory Comput., 2, 815–826. https://doi.org/10.1021/ct050289g
- Vreven, T., Morokuma, K., Farkas, Ö., Schlegel, H. B., & Frisch, M. J. (2003). Geometry optimization with QM/MM, ONIOM, and other combined methods. I. Microiterations and constraints. J. Comput. Chem., 24, 760–769. https://doi.org/10.1002/jcc.10156
- Waterhouse, A., Bertoni, M., Bienert, S., Studer, G., Tauriello, G., Gumienny, R., ... Schwede, T. (2018). SWISS-MODEL: Homology modelling of protein structures and complexes. Nucleic Acids Research, 46, W296–W303. https://doi.org/10.1093/nar/ gky427
- Weiner, P. K., & Kollman, P. A. (1981). AMBER: Assisted model building with energy refinement. A general program for modeling molecules and their interactions. J. Comput. Chem., 2, 287–303. https://doi.org/10.1002/jcc.540020311

- Xue, T., Do, M. T. H., Riccio, A., Jiang, Z., Hsieh, J., Wang, H. C., ... Yau, K.-W. (2011). Melanopsin signalling in mammalian iris and retina. *Nature*, 479, 67–73. https://doi.org/10.1038/nature10567
- Yanai, T., Tew, D. P., & Handy, N. C. (2004). A new hybrid exchange-correlation functional using the Coulomb-attenuating method (CAM-B3LYP). Chemical Physics Letters, 393, 51–57. https://doi.org/10.1016/j.cplett.2004.06.011
- Zhu, S., Brown, M. F., & Feller, S. E. (2013). Retinal Conformation Governs p *K* a of Protonated Schiff Base in Rhodopsin Activation. *J. Am. Chem. Soc.*, *135*, 9391–9398. https://doi.org/10.1021/ja4002986